

Evaluation of cellular structures with triply periodic minimal surfaces fabricated by additive manufacturing

André Oliveira

IDMEC, Instituto Superior Técnico, Universidade de Lisboa, Lisboa, Portugal
(andreoliva853@hotmail.com)

Luís Reis

IDMEC, Dep Eng Mecânica, Instituto Superior Técnico, Universidade de Lisboa, Portugal
(luis.g.reis@tecnico.ulisboa.pt) ORCID [0000-0001-9848-9569](https://orcid.org/0000-0001-9848-9569)

Marco Leite

IDMEC, Dep Eng Mecânica, Instituto Superior Técnico, Universidade de Lisboa, Portugal
(marcoleite@tecnico.ulisboa.pt) ORCID [0000-0002-0319-4475](https://orcid.org/0000-0002-0319-4475)

Frederico Alves

Instituto Superior Técnico, Universidade de Lisboa, Portugal (frederico.alves@tecnico.pt)
ORCID [0000-0003-0848-4348](https://orcid.org/0000-0003-0848-4348)

Augusto Moita de Deus

CEFEMA, Dep Eng Mecânica, Instituto Superior Técnico, Universidade de Lisboa, Portugal
(amd@tecnico.ulisboa.pt) ORCID [0000-0002-0451-6245](https://orcid.org/0000-0002-0451-6245)

Manuel Sardinha

IDMEC, Dep Eng Mecânica, Instituto Superior Técnico, Universidade de Lisboa, Portugal
(manuel.r.sardinha@tecnico.ulisboa.pt) ORCID [0000-0003-2124-8569](https://orcid.org/0000-0003-2124-8569)

M. Fátima Vaz

IDMEC, Dep Eng Mecânica, Instituto Superior Técnico, Universidade de Lisboa, Portugal
(fatima.vaz@tecnico.ulisboa.pt) ORCID [0000-0003-1629-523X](https://orcid.org/0000-0003-1629-523X)

Author Keywords

Cellular structures, triply periodic minimal surfaces, additive manufacturing.

Type: Rapid communication

 Open Access

 Peer Reviewed

 CC BY

Abstract

Cellular structures are formed by struts and edges, which makes them difficult to fabricate by conventional technologies. The emergence of 3D printing has enabled the production of such complex structures. In the present work, the Fused Filament Fabrication method was used to obtain cellular structures formed by the repetition of triply periodic minimal surfaces unit cells. Due to the complexity of the cells, several defects occurred until the procedure was fine-tuned. Failure analysis of samples was performed after bending and compression tests. Failure occurs at the same locations of the samples independently of their relative density, for the three densities tested. These fracture initiation locations correspond to the zones where the von Mises stress is highest.

1. Introduction

Cellular materials are made of networks of struts or plates with two-dimensional (2D) or three-dimensional (3D) arrangements. For example, 2D cellular solids include honeycombs, and in the case of 3D cellular structures, one can have randomly oriented cells (foams) or a periodic repetition of a unit cell (lattices). When compared to compact materials, cellular structures display high values of the mechanical properties scaled to their relative density, such as specific strength, stiffness and energy absorption, while maintaining low weight. This makes

them adequate choices for use in medical implants and for lightweight aerospace and automotive components (Kumar et al. 2020; Benedetti et al. 2021). Another example of the common use of cellular materials is the core of sandwich panels (Araújo et al. 2019; Miranda et al. 2021).

Recently, there has been a growing interest in truss lattice structures (Monteiro et al. 2021). These meta-materials, or architected cellular materials, allow obtaining controlled mechanical properties by tailoring the geometrical design parameters. There are several types of unit cells that can be used to design lattice structures, such as atomic-based arrays, Kelvin and rhombicuboctahedron, pyramidal, diamond cubic or octahedral (Benedetti et al. 2021).

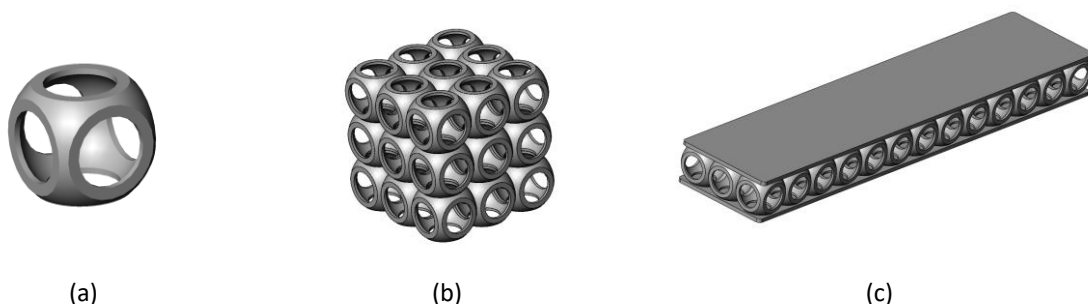
Triply periodic minimal surfaces (TPMS) have emerged as an example of cellular structures inspired by natural materials (Kumar et al. 2020). Recently, TPMS have been applied to mimic bone structure as they can have a mean curvature that resembles the one of trabecular bone (Zhou et al. 2020).

The present work aims at tuning the parameters of the Fused Filament Fabrication (FFF) method to obtain complex lattices structures formed by TPMS unit cells. Several drawbacks were overcome. Examples of cubic and plate structures were experimentally tested under compression and bending, for three relative densities. Experimental results were compared with finite element analysis. A failure analysis was also conducted.

2. Materials and Methods

All the samples were designed with the 3D CAD program SolidWorks® (SolidWorks, 2019). The unit cell studied in the present work had resemblance to the one proposed by Kumar et al. (2020). These authors considered a bioinspired unit cell that mimics a sea urchin shape. In the present work, the unit cell was constructed from a hollow sphere, modified with the opening of circular holes. Thus, the unit cell (Figure 1a) does not exhibit an additional curvature, in comparison with the unit cell of Kumar et al. (2020). The detailed drawing procedures can be found in the work of Oliveira (2021).

One of the most important parameters of cellular solids is their relative density, which is the ratio of the volume occupied by the solid divided by the volume of the entire unit cell. In the present work, unit cells with three relative densities, namely 0.2, 0.25 and 0.3 were evaluated. The volume that encloses the unit cell is a cube with 13.5 mm side. Cubic compression specimens (Figure 1b) and sandwich panel samples (Figure 1c) were constructed using repetitions of the unit cells. For example, Figure 1b) exhibits a repetition of three cells in each axis, while the panel of Figure 1c) has 13 unit cells along its length and 3 unit cells along its width. The thickness of the face-sheets is equal to 1.5 mm.



(a) (b) (c)
Figure 1: Schematics of: (a) unit cell with a relative density of 0.2; (b) cubic array and (c) core of sandwich panel

The specimens were manufactured using the FFF technology, in a Ultimaker 3 machine. The CAD models were created in Solidworks and exported as STL files. In the slicing software, in

this case, the Ultimaker CURA version 4.11.0 (Ultimaker, the Netherlands), the model is sliced into layers, and the G-code is generated, giving the instructions to the 3D printing machine.

The material used was the polylactic acid neutral (PLA-N), supplied by Filkemp, Portugal. The samples were printed with an infill of 100%, a layer height of 0.2 mm, a line width of 0.35 mm, a printing temperature of 200°C, a build temperature of 60°C and a nozzle diameter of 0.4 mm. Additionally, several slicing parameters were evaluated, and iterations were performed to improve the surface quality of the specimens and promote an adequate adhesion between cells. Among the tuned parameters, the scaling factor, travel acceleration and activation of “z-hop” and “avoid printed parts” were identified as influential.

For each relative density, three parts were printed to obtain compression and bending samples, in order to perform three tests under the same conditions. The compression and 3PB (three-point bending) tests were performed in an Instron 3369 machine, with a load cell of 50 kN and a cross-head speed of 2.5 mm/min, in accordance with the standards ASTM D1621 – 16 and ASTM C393 – 00, respectively.

The numerical simulations were performed using NX Nastran (version 2019.1) with Siemens NX (version 1957) as pre and post-processor. A mesh with CTETRA(10) elements was used both in the compression and the 3PB simulations. A mesh refinement study was undertaken and element sizes of 1 mm were selected. A maximum displacement of 3 mm was applied in the compression tests and in the flexural tests. Simulations were performed under elastic conditions.

3. Results and Discussion

Figure 2a)-c) presents some defects identified and addressed during the iteration process described above. Even if an improvement was possible to achieve with the adjustment of process parameters, smaller defects were still found in the final samples. Some of the major concerns with the tested samples were related with overhangs related defects, stringing between cells and lack of manufacturing repeatability. Often, the test samples failed during the printing process when half the cell of a sample was reached. This was mostly due to the small cross-sectional area (“struts”) of each cell at such moments. To address the problem, the travel acceleration was decreased from a standard 5000 mm/s⁻² to 3250 mm/s⁻² and the print acceleration was reduced from 5000 mm/s⁻² to 4000 mm/s⁻², which allowed for an improved control of the extrusion process of small sections. Even so, reducing speed and acceleration made the bridging ability of the cells more difficult, which promoted the existence of overhangs. These are found when the extrusion head reaches the upper section of the cells and the new layers are only partially supported by the previous layer, creating irregularities in the unsupported section of the unit cells.

Another solution implemented was adding the “Avoid printed parts” and “Z-hop” parameters in the slicing software. The travel avoid distance was set equal to 3.0 mm, while Z-hop height was 2.0 mm. Adding both parameters assures that the extrusion head moves around the material already deposited to avoid new filaments to adhere to the part itself. These parameters also helped to diminish the strings shown in Figure 2b) and to mitigate the print failures. Figure 2c) presents the failed prints of the three samples with different scale sizes. It happened due to the small dimension of the samples. Increasing dimensions of the samples also addressed the small section problem identified above. Figure 2d) shows a much smoother and more precise specimen.

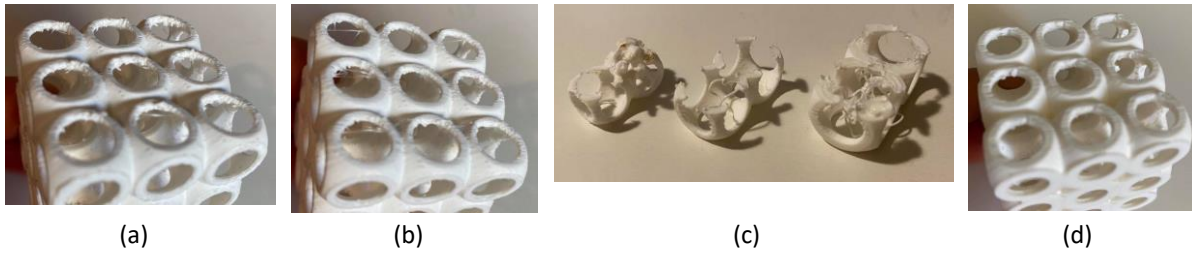


Figure 2: Examples of defects during 3D printing: (a) curly filaments in the top of the holes due to overhang; (b) strings inside the part; (c) different scale factors; (d) a sample with few defects

Figure 3a)-c) presents an example of a compression test. After an elastic linear regime, the layer of cells in contact to the upper plate starts to collapse, after which the collapse happens at the bottom layer and finally there is the crushing of the middle layer. Fracture occurs at the middle of the struts. This is in accordance with finite element analysis, which shows that the maximum von Mises stress was concentrated at the middle of the struts (Figure 3c)). In the present work, the mode of deformation was the horizontal cell layer collapse, which differs from the results of Kumar et al. (2020) where collapse occurs in layers that make 45° angles with the direction of the applied load.

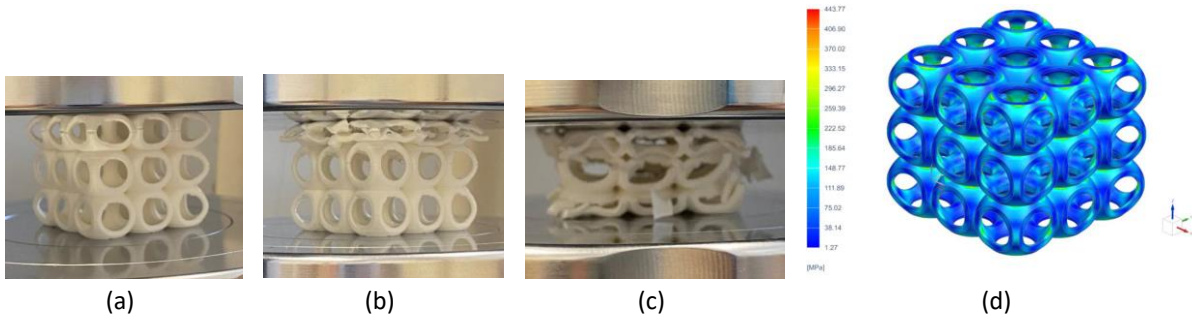


Figure 3: (a)-(c) Three steps of an experimental compression test; (d) von Mises stress obtained with finite element analysis

Figure 4 shows the beginning of fractures in several spots of the unit cells during bending tests. Collapse starts to occur at the same height of the cells, almost along the same line (Figure 4a)). The failure along one line (Figure 4b)) is possibly associated with the presence of defects, probably related to overhangs.

From the experimental tests, it was possible to determine the slope, K , of the load-displacement curve at the elastic zone and the absorbed energy, E_a until failure. Both compression and 3PB tests revealed that the increase of the relative density lead to an increase of the stiffness and the absorbed energy as indicated in Table 1. The finite element results of stiffness and absorbed energy (Table 1) were found to be much higher than the experimental ones, probably due to the presence of defects in the samples.

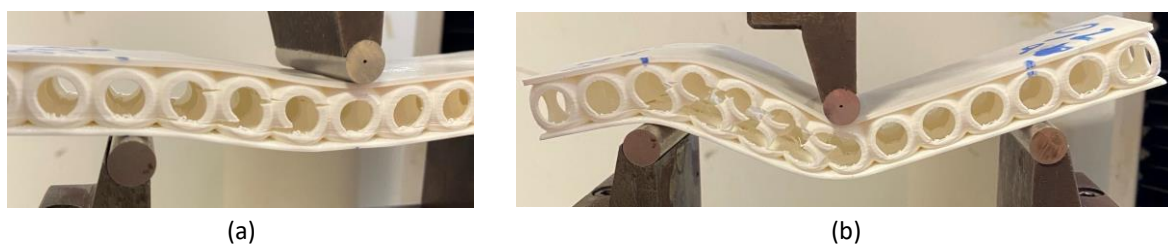


Figure 4: Two steps of an experimental 3PB test

Table 1: Experimental results calculated for compression and bending tests

	Experimental			Simulations	
	Relative density	Stiffness [N/mm]	Absorbed energy [J]	Stiffness [N/mm]	Absorbed energy [J]
Compression	0.2	1715 ±310	6.12±1.32	5708	25.69
	0.25	1924±117	7.41±1.71	7605	34.22
	0.3	2606±148	14.67±1.68	10669	48.01
Bending	0.2	312±22	0.94±0.19	437	1.97
	0.25	333±20	1.69±0.06	499	2.25
	0.3	356±15	3.44±0.05	582	2.62

The model used is not able to capture all the phenomena occurring during the experimental procedure, such as delamination.

4. Conclusions

Cellular structures often have intricate geometric characteristics, which impose manufacturing difficulties. Even if the development of additive manufacturing technologies has made possible the production of increasingly more complex cellular parts, producing TPMS structures with good quality is still challenging. This work evaluated and addressed the defects such as stringing and overhang present in FFF lattice structures with TPMS unit cells. Due to fine-tuning of the process, it was possible to obtain samples with acceptable quality. Specimens were tested under compression and bending. Experimental and numerical results follow the same trends, although there are discrepancies in the values. One may conclude that the results were possibly affected by the presence of inner defects that were not previously considered in the numerical simulations. Failure occurs at the same locations of the samples independently of their relative density, for the three densities tested. Moreover, the origin of the failure is related with the location of identified macroscopic defects.

References

- Araújo, H., M. Leite, A. R. Ribeiro, A. M. Deus, L. Reis, and M. Fátima Vaz. 2019. "The effect of geometry on the flexural properties of cellular core structures". *Proceedings of the Institution of Mechanical Engineers, Part L: Journal of Materials: Design and Applications* 233, no. 3: 338-47. <https://doi.org/10.1177/1464420718805511>.
- Benedetti, M., A. du Plessis, R. O. Ritchie, M. Dallago, S. M. J. Razavi, and F. Berto. 2021. "Architected cellular materials: A review on their mechanical properties towards fatigue-tolerant design and fabrication". *Materials Science and Engineering: R: Reports* 144: Article number 100606. <https://doi.org/10.1016/j.mser.2021.100606>.
- Kumar, A., L. Collini, A. Daurel, and J.-Y. Jeng. 2020. "Design and additive manufacturing of closed cells from supportless lattice structure". *Additive Manufacturing* 33: Article number 101168. <https://doi.org/10.1016/j.addma.2020.101168>.
- Miranda, A., M. Leite, L. Reis, E. Copin, M. F. Vaz, and A. M. Deus. 2021. "Evaluation of the influence of design in the mechanical properties of honeycomb cores used in composite panels". *Proceedings of the Institution of Mechanical Engineers, Part L: Journal of Materials: Design and Applications* 235, no. 6: 1325-40. <https://doi.org/10.1177/1464420720985191>.
- Monteiro, J. G., M. Sardinha, F. Alves, A. R. Ribeiro, L. Reis, A. M. Deus, M. Leite, and M. Fátima Vaz. 2021. "Evaluation of the effect of core lattice topology on the properties of sandwich panels produced by additive manufacturing". *Proceedings of the Institution of Mechanical Engineers, Part L: Journal of Materials: Design and Applications* 235, no. 6: 1312-24. <https://doi.org/10.1177/1464420720958015>.

Oliveira, A. 2021. "Design and analysis of bio-inspired cellular structures with variable relative density produced with fused filament fabrication". Master's thesis, Instituto Superior Técnico, Universidade de Lisboa. <https://fenix.tecnico.ulisboa.pt/cursos/memec/dissertacao/1691203502344756>.

Zhou, H., M. Zhao, Z. Ma, D. Z. Zhang, and G. Fu. 2020. "Sheet and network based functionally graded lattice structures manufactured by selective laser melting: Design, mechanical properties, and simulation". *International Journal of Mechanical Sciences* 175: Article number 105480. <https://doi.org/10.1016/j.ijmecsci.2020.105480>.

Acknowledgments

This work was supported by FCT, through IDMEC, under LAETA, Project UIDB/50022/2020. M. Leite and L. Reis gratefully acknowledge the funding of the BigFDM project, FCT Reference PTDC/EME-EME/32103/2017.